Diyala Journal of Engineering Sciences, Vol. 11, No. 2, June 2018, pages 42-48 ISSN 1999-8716
DOI: 10.24237/djes.2018.11205 eISSN 2616-6909

Studying the Strength of the Pile Cap Concrete Simulated as a Continues Deep Beam using Self Compact Concrete

Zouhear A. Hachem
Department of Highway and Transporting Engineering, College of Engineering, Al-Mustansiriya University

Abstract

This paper is an experimental study to investigate the effect of concrete compressive strength on the structural behavior of continuous reinforced concrete deep beams to utilize the results on the piles caps works. Three nominal concrete compressive strengths 50, 60 and 70 MPa obtained by self-compacting concrete were frequently used with four groups of shear span-to-depth ratios 5.71, 1.25, 1.08 and 0.95 to produce twelve continuous beams; three of them are shallow and the rest are deep. The comparisons were designed to reveal the variation in the structural behaviors among the shallow and deep specimens from a side, and among the deep specimen from another side.
The experimental program concentrated on the ultimate strength, load-deflection curve, cracking and failure mode of the specimens. The results revealed that the concrete compressive strength is an effective factor on the behavior of the deep beam and when its value increased the ultimate strength and the serviceability of specimen can be improved about 48% whilst the enhancement achieved in shallow beams about 9%. The percentage of the obtained improvement for a specimen can be increased by decreasing its shear span-to-depth ratio.

Keywords: Pile cap, deep beam, shallow beam, depth ratio, and self-compacting concrete.

Paper History: Received: (15/6/2016), Accepted: (29/12/2016)

1.Introduction

A pile cap, shown in Figure 1, is a stocky reinforced structure which spreads and distributes the load from a column or bridge pier downwards into supporting piles [1]. Whilst, the deep beam is a structural member whose behavior is dominated by shear deformations. In practice, engineers typically encounter deep beams when designing transfer girders, bridge bents, or pile supported foundations as well [2, 3]. Continuous deep beams occur as transfer girders in multi-story frames, as foundation wall structures and as pile caps etc. The usual design practice for continuous deep beams has been to employ empirical equations, which are invariably based on simple span deep beam tests. Given the unique behavioral pattern of a continuous deep beam, his practice is unreliable [4].

Figure 1: Pile Caps Behave as Continuous Deep Beams

Some provisions are adopted to determine if beam is deep or shallow (slender). If the beam behaves as shallow, its failure mode can be transformed to flexural deformations, however, force transfer in continuous deep and shallow beam is cleared in Figure 2. When the following expressions achieve, lead to deep beam behavior:

$a/d < 2 – 2.5$ … (1) [2]
$a/h < 2$ … (2) [5, 6]
$l_c/h \leq 4$ … (3) [5-8]

Where:
a: Shear span of a beam.
d: Distance between the extreme compression fiber and centroid of tension reinforcement.
h: Overall depth or height of the beam.
l_c: Face-to-face distance between the two supports of the beam.

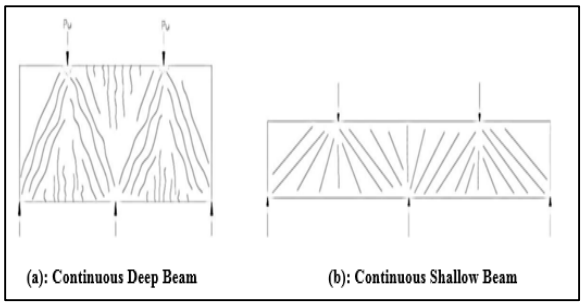

Figure 2: Comparison of Force Transfer between the Two Continuous Beams [4]

2. Research Significance

This paper investigates the effect of concrete compressive strength (f'_c) with different shear span-to-depth ratio (a/d) on the behavior of continuous reinforced concrete deep beams in order to reflect the results into reinforced concrete pile caps functions. The ultimate load (P_u), flexural deflection (Δ), cracking load (P_{cr}) and crack pattern of tested continuous deep beam are focused and compared with ones in corresponding continuous shallow beams to obtain significant conclusions.

3. Test Program

Twelve reinforced concrete beams with different configurations are the specimens of the work; three of them are shallow and the rest are deep. Table 1 contains the differences among the beams in terms of compressive strength (f'_c) and span-to-depth ratio (a/d).

Table 1 Configurations of the Tested Beams.

Group	Symbol	Nominal f'_c (MPa)	a (mm)	d (mm)	a/d
Shallow Beams	B1	50	400	70	5.71
	B2	60			
	B3	70			
Deep Beams	B4	50		320	1.25
	B5	60			
	B6	70			
	B7	50		370	1.08
	B8	60			
	B9	70			
	B10	50		420	0.95
	B11	60			
	B12	70			

3.1 Concrete

Self-compacting concrete (SCC) is used in this work due to its regarding homogeneity and compaction within intricate structures and to improve the overall strength, durability and quality of concrete [9]. Ordinary Portland cement type I was used. The coarse aggregate was a 14 mm maximum size crushed gravel with specific gravity and absorption of 2.64 and 0.57%, respectively and the fine aggregate was natural river sand with a 3.18 fineness modulus with specific gravity and absorption of 2.7 and 1.5% respectively. For SCC production, A fine limestone powder (LSP) with fineness (3100 cm²/gm) is used to avoid excessive heat generation, enhance fluidity and cohesiveness and the water content of the mix is reduced by using a superplasticizer (SP) complies with ASTM C 469–86 [10]. The mix proportions and the average results of cylinder strength (f'_c) for all beams are given in Table 2.

Table 2 Mix Proportions and Compressive Strength of SCC Concrete.

Mix.	Nominal f'_c (MPa)	Tested f'_c (MPa)	Cement (kg/m³)	LSP (kg/m³)	Sand (kg/m³)	Gravel (kg/m³)	Water (liter/m)	SP (liter/m)
1	50	49.6	300	200	780	870	200	7.0
2	60	62.4	400	150	770	870	198	6.0
3	70	71.8	450	100	756	870	165	10.0

3.2 Reinforcement

Deformed steel bars of diameter 10 mm were used for the main reinforcement and plain steel bars of diameter 4 mm were used for engaging the main reinforcement and as vertical and horizontal web reinforcements. Properties of the steel bars are shown in Table 3. The spacing of web and main reinforcements were adopted according to ACI Code 318–08 [5] and designed to be near its minimum limits.

Table 3 Properties of Reinforcing Steel.

Diameter of Bar Ø (mm)	Yield Stress f_y MPa	Ultimate Stress f_u MPa	Modulus of Elasticity E_s GPa
4	317.1	418.3	200
10	494.7	589.8	200

3.3 Specimens Details

Two types of specimens are cast; shallow and deep beams. All the beams are the same in length of 1100 mm, width of 100 mm, main reinforcement of 2Ø10 mm and loading with supporting, as shown in Figure 3 below. The main difference among the beams is the overall depth (h) which governs ratio of beam deepness through a/d ratio, for the shallow beam one value of h was used and equals 100 mm, but for the deep beams there are three values of (h) which were 350, 400 or 450 mm. Other difference between the types of the beams is the web reinforcement to resist the shear stresses, in the deep beams the web reinforcements consists of (12 vertical and 4 horizontal) stirrups of Ø4 mm, whilst the web reinforcement in the shallow beams consists of 12 vertical stirrups of Ø4 mm only.

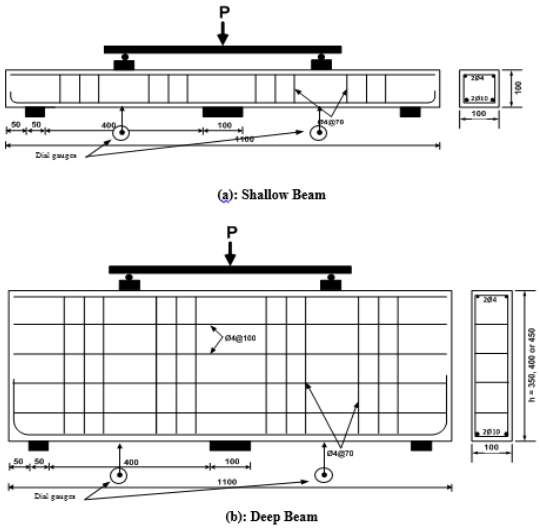

Figure 3: Details of the Beams (all dimensions are in mm)

3.4 Test Procedure

Before testing, a thin layer of white emulsion paint was applied onto the surface of the specimen to aid the cracks detection. The dial gages were positioned at the bottom of midspan of each span of the beam. All the beams were tested by loading at midspan as in Figures 3 and 4. Loading was applied in increments of 5 kN to record the deflection and detect the cracking. Testing was continued until the beam showed a drop in load carrying capacity.

Figure 4: Beam at the Test

4. Test Results

The main results which are listed in Table 4 will be discussed according to the compressive strength (f'_c) and span-to-depth ratio (a/d) and divided into the below topics.

Table 4 Results of the Tested Beams.

Group	Beam	P_{cr} (kN)	P_u (kN)	P_{cr} / Pu (%)	Δ_{max} (mm)	Failure Mode
Shallow	B1	20	90	22	3.28	flexure
	B2	28	95	29	2.84	flexure-shear
	B3	38	98	39	2.73	flexure-shear
Deep	B4	180	640	28	2.95	shear
	B5	180	695	26	2.81	shear
	B6	215	715	30	2.7	shear
	B7	215	710	30	2.89	shear
	B8	230	720	32	2.77	shear
	B9	275	745	37	2.67	shear
	B10	225	886	25	2.73	shear
	B11	240	900	27	2.65	shear
	B12	315	945	33	2.58	shear

4.1 Ultimate Strength

The ultimate load which represents the failure of the tested beam (P_u) mentioned in Table 4 reflects the ultimate strength. Figure 5 shows the gradual increase in the beams ultimate strength through B1 to B12. The gradual increase of P_u in the shallow beams (B1, B2 and B3) came from f'_c increase (50 – 70 MPa) in the three beams respectively with constant a/d ratio (5.71), and the P_u of B3 increased about 9% in comparison with P_u of B1 (90 kN).

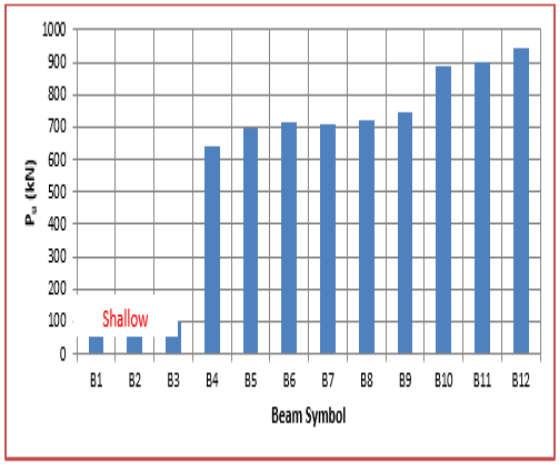

Figure 5: Ultimate Strengths of the Tested Beams

However, the achieved increase in P_u in the deep beams came from increase of f'_c in three different a/d ratios. When both f'_c increase up to 70 MPa and a/d decrease to 0.95, more increase in P_u can be gained; therefore B12 was strongest beam and its P_u achieved enhancement of 48% in comparison with P_u of B4 (640 kN). For the same value of a/d in one group, the P_u of the beams can be increased by f'_c increase and that is achieved where B6, B9 and B12 (with maximum f'_c value of 70 MPa) are the strongest of their groups and this result confirmed by the results of Birrcher et al. [2].

On other hand, continuous decreasing in a/d leads to enhance P_u of the deep beams against the shallow beams, therefore (B4 – B12) have ultimate strengths greater than that of (B1 – B3) and this results can be applied on continuous deep beams and simply supported deep beams [4]. Furthermore, it can be concluded that the activity of enhancing P_u by increasing f'_c value in deep beams (up to 48%) is better than its increasing in shallow beams (9%).

It is important to determine the activity of f'_c increase on enhancing P_u of deep beams through a/d decreasing ratios, so that Figure 6 was graphed according to B4 (increment in P_u = 0) to explain this aim. Figure 6 revealed that a/d is very effective for raising the activity of f'_c on enhancing P_u of continuous deep beams, thereby, the percent increment of P_u according to less a/d (0.95) reaches about 38, 41 and 48 % for f'_c varied from 50 up to 70 MPa respectively, while the percent increment of P_u according to greater a/d ratio (1.25) is less than and about 10%.

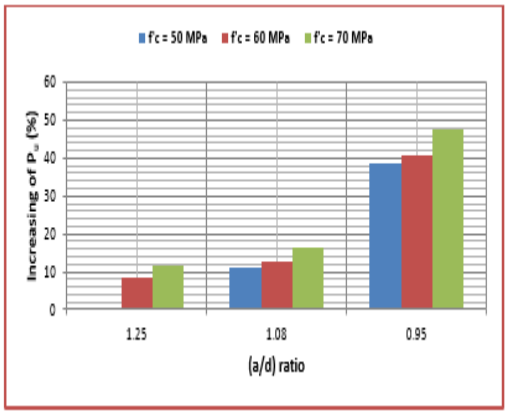

Figure 6: Ultimate Strengths Enhancement of the Tested Deep Beams

4.2 Load-Deflection Behavior

It is obvious from Figure 7, the similarity in behavior among the curves of all beams and characterized by a nearly bilinear response. After flexural cracking appear, a second, softer linear region was observed in all of deep beams curves up to the failure; this behavior observed in previous researches [11, 12], however, the load-deflection curves of the shallow beams seem flat due to their low strength in comparison with the ultimate strength of the associated deep beams in the same graph. Other important matter is the homogeneity of curves with absence of scattered or many singular points and that reflects the reliability of behavior obtained from using SCC in casting the tested beam.

Figure 7 clarifies two notes; the first is that the deflections of the deep beams is fewer that corresponding deflections of the shallow beams in all stages of loading to reflect expected highest stiffness of the deep beams due to their high moment of inertia comes from the tall depth against the shallow beams. The second note is that the shallow beam exhibit deflections at failure greater than the ones of deep beams at their failure; whatever this results confirms the effect of a/d ratio in reducing the deflection of the deep beams at failure stage.

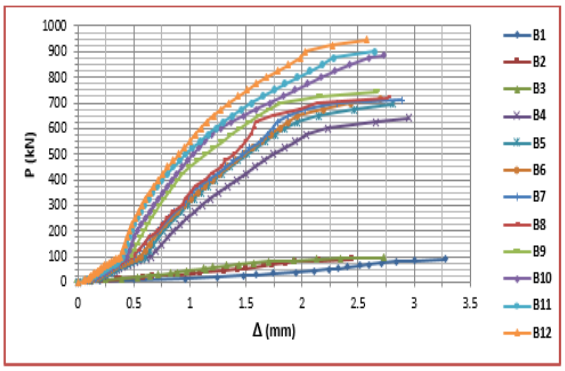

Figure 7: Load-Deflection Behavior of the Tested Beams

The investigation of f'_c increase activity according to a/d decrease on the load-deflection behavior of the deep beams need to graph Figure 8 which confirms defective of f'_c increase or a/d decrease on the general load-deflection behavior of all tested deep beams.

The graphic curves according to f'_c increase confirm expected increase of stiffness with the f'_c increment for each a/d ratio. Also, Figure 8 shows decrease in deflections and increase of the beam stiffness according to a/d decrease for each constant value of f'_c. The results lead to conclude that a/d ratio is effective for the activity of f'_c on moment of inertia value and increase the stiffness to govern deflections and flexural serviceability.

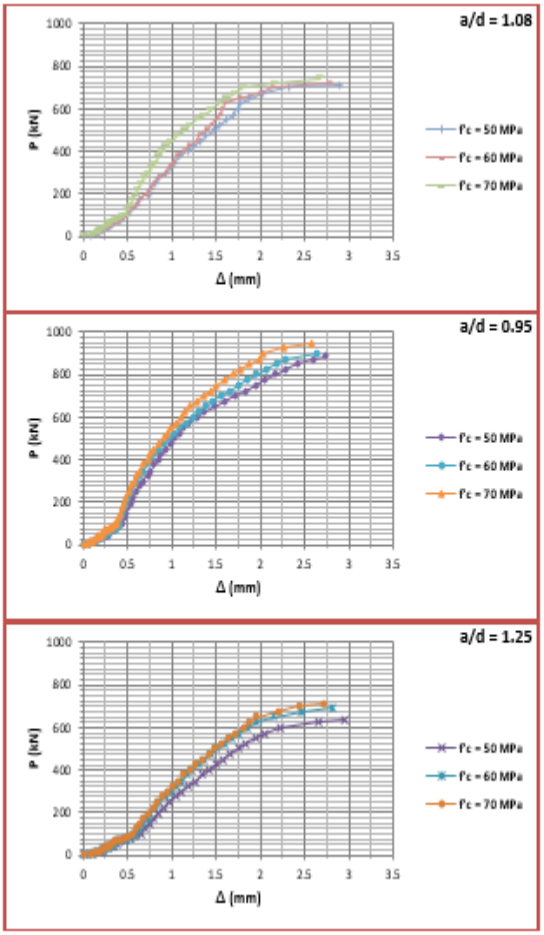

Figure 8: Load-Deflection Behavior of the Tested Deep Beams

From ultimate strength and load-deflection behavior topics; the results indicate the advantages of using SCC and increasing its f'_c in design and working with piles cap, but increasing the depth of the section to decrease a/d ratio is more preferable option to achieve these advantages in high percentage.

4.3 Cracking and Failure Mode

Cracking patterns exhibited by the shallow beams specimens are shown in Figure 9. After formation of the first flexural crack at midspan at loads (P_{cr}) about 22 – 39% of P_u, diagonal cracks formed in the general direction between supports and load points on the test. Intermediate flexural cracks between the midspan and the supports inclined through its heightening toward the load points to be flexure-shear after that. In spite of flexure-shear cracks presence, B1 failed by midspan flexural crack, whilst B2 and B3 failed by the flexure-shear cracks due to their high f'_c (60 – 70 MPa) respectively in resisting flexure.

All the deep beams showed a same response of cracking patterns up to failure. In the early steps of loading, few vertical flexural cracks formed in the midspan regions at P_{cr} / P_u = 25 – 37%. As the load increased diagonal cracks appeared and propagated rapidly toward the outside edge of the loaded point and the inside edge of the support. While the diagonal cracks were developing across length, their widths were propagating in the center of shear span, as shown in Figure 9. The cracking Pattern of the present work complies with previous experimental works [2] except for P_{cr} / P_u = 50% [4], 30 – 50% [13] and 25% [14]. The failure in the present work characterized by widening the web shear cracks that extended between the outside edge of the loaded point and the inside edge of the support.

Figure 9: Cracking Patterns of the Tested Beams

The cracking loads of the tested beams (P_{cr}) mentioned above in Table 4 reflects the exceeding of tensile stresses caused by external loading for the tensile strength of the section which depending mainly on f'_c value. Figure 10 shows the gradual increase in the beams cracking load through B1 to B12. The gradual increase of P_{cr} in the shallow beams of f'_c increase (50 – 70 MPa) in the three beams respectively with constant a/d ratio (5.71), and the P_{cr} of B3 increased about 90% in comparison with P_{cr} of B1 (20 kN).

However, the achieved increase in P_{cr} of deep beams groups is depended on f'_c in three different a/d ratios. When both f'_c increase up to 70 MPa and a/d decrease to 0.95, more increase in P_{cr} can be gained; therefore B12 was last cracked beam and its P_{cr} increased about 75% in comparison with that of B4 (180 kN). For the same value of a/d in one group, the P_{cr} of the beams can be increased by f'_c increase and that is achieved where B6, B9 and B12 (with maximum f'_c value of 70 MPa) are the last cracked beams in their groups as shown in Figure 11.

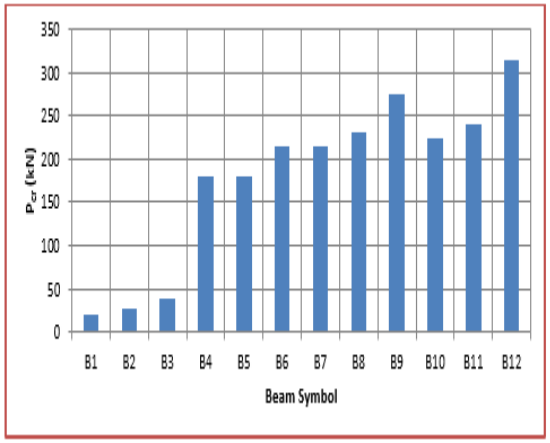

Figure 10: Cracking Loads of the Tested Beams

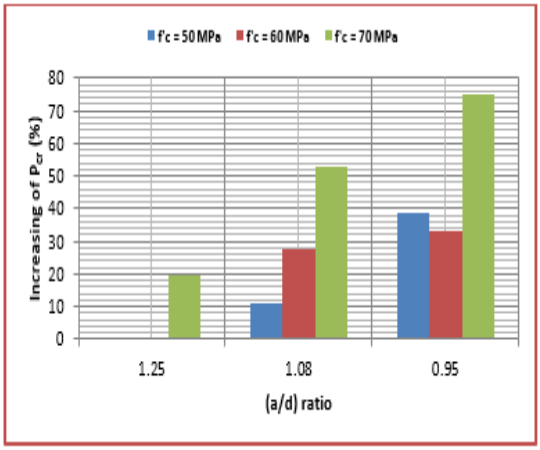

Figure 11: Cracking Loads Enhancement of the Tested Deep Beams

Furthermore, it can be noticed that increasing the f'_c to enhance P_{cr} of the deep beams which increased up to 75% in the present work is less than that enhancement achieved in shallow beams which was 90% even when decreasing a/d ratio in deep beams raising the activity of increasing the f'_c.

5. Conclusions

- Increasing the compressive strength of concrete is a successful method for enhancing the ultimate strength and capacity of the piles cap when it designed as deep beam.
- The activity of the compressive strength of concrete on enhancing the ultimate strength and cracking load of deep beams can be magnified from 10 – 38% and from 19 – 75% respectively when the depth ratio (a/d) decreased from 1.25 to 0.95.
- The enhancement of the ultimate strength by increasing the compressive strength value in deep beams can be raised up to 48% and it is better than increasing in shallow beams where the increment is about 9%.
- The enhancement of the cracking load by increasing the compressive strength value in deep beams can be raised up to 75% but it is less than increasing in shallow beams where the increment is about 90%.
- For ultimate strength and flexural stiffness of deep beams; the results indicate the advantages of using the self-compacting concrete and increasing its compressive strength in design and working with piles cap, but increasing the depth of the section to decrease a/d ratio is more preferable option to achieve these advantages in high percentage.
- Through the ability of increasing the compressive concrete strength for increasing stiffness to reduce deflection and the ability of this increment for delaying cracking appearance, it is no doubt, the deep beams and piles cap exhibit more serviceability with high strength concrete.

6. References

[1] Adebar P., Kuchma D., and Collins M. P. Strut-And-Tie Models for the Design of Pile Caps: An Experimental Study, ACI Structural Journal, Jan-Feb, 87,(1), (1990), 81-92.

[2] Birrcher D., Tuchscherer R., Huizinga M., Bayrak O., Wood S., and Jirsa J., Strength and Serviceability Design of Reinforced Concrete Deep Beams, Center for Transportation Research, the University of Texas, (2009), 400.

[3] Al-Sarraf S. Z., Al-Shaarbaf I. A. S. and Diab A. S., Effect of Steel Fiber on the Behavior of Deep Beams with and without Web Opening, Eng. & Tech. Journal, 29, (1), (2011), 19.

[4] Singh B., Kaushik S. K., Naveen K. F. and Sharma S., Design of a Continuous Deep Beam Using the Strut and Tie Method, Asian Journal of Civil Engineering (Building And Housing), 7, (5), (2006), 461-477.

[5] ACI Committee 318, Building Code Requirements for Structural Concrete (ACI318-08) and Commentary (ACI318R-08),

American Concrete Institute, Farmington Hill, Michigan (2008), 471.

[6] Shahidul Islam S. M., Automated Design of Reinforced Concrete Deep Beams, Ph.D. Thesis, School of Engineering and Information Technology, University of New South Wales, Canberra, 2012, 285.

[7] Seo, S. Y., Yoon S. J. and Lee W. J., Structural Behavior of RC Deep Beam with Headed Longitudinal Reinforcements, 13th World Conference on Earthquake Engineering Vancouver, B.C., Canada, (58), August 1-6, 2004, 12.

[8] Nagarajan P., and Pillai M. T. M., Development of Strut and Tie Models for Simply Supported Deep Beams Using Topology Optimization, Songklanakarin Journal of Science and Technology, 30, (5), Sep. – Oct. (2008), 641-647.

[9] Campion, J. M., and Jost, P., Self-Compacting Concrete: Expanding the Possibility of Concrete Design and Placement, ACI Concrete International, 22, (4), April 2000, 31-34.

[10] ASTM Designation C494–86, Chemical Admixtures for Concrete, Annual Book of ASTM Standards 1989, 04, (2), 248–255.

[11] Aguilar G., Matamoros A. B., Parra-Montesinos G. J., Ramírez Julio A. and Wight J. K., Experimental Evaluation of Design Procedures for Shear Strength of Deep RC Beams, ACI Structural Journal, 99, (4), Jul-Aug. (2002), 539-548.

[12] Roy N. C. and Breña S. F., Behavior of Deep Beams with Short Longitudinal Bar Anchorages, ACI Structural Journal, 105, (4), Jul-Aug. (2008), 460-470.

[13] Arabzadeh A., Aghayari R. and Rahai A. R., Investigation of Experimental and Analytical Shear Strength of Reinforced Concrete Deep Beams, International Journal of Civil Engineering, 9, (3), Sep. (2011), 207-214.

[14] Quintero-Febres C. G., Parra-Montesinos G. and Wight J. K., Strength of Struts in Deep Concrete Members Designed Using Strut-and-Tie Method, ACI Structural Journal, 103, (4), Jul-Aug. (2006), 577-586.